Structural, transport, magnetic, and thermal properties of $Eu_8Ga_{16}Ge_{30}$

S. Paschen, W. Carrillo-Cabrera, A. Bentien, V. H. Tran,* M. Baenitz, Yu. Grin, and F. Steglich
Max Planck Institute for Chemical Physics of Solids, Nöthnitzer Straße 40, D-01187 Dresden, Germany
(Received 9 May 2001; published 1 November 2001)

$Eu_8Ga_{16}Ge_{30}$ is the only clathrate known so far where the guest positions are fully occupied by a rare-earth element. Our investigations show that, in addition to the previously synthesized $Eu_8Ga_{16}Ge_{30}$ modification with clathrate-I structure, there exists a second modification with clathrate-VIII structure. Polycrystalline samples of both phases behave as local-moment ferromagnets with relatively low Curie temperatures (10.5 and 36 K). The charge-carrier concentrations are rather small (3.8 and 12.5×10^{20} cm^{-3} at 2 K) and, together with the low Curie temperatures, point to a semimetallic behavior. Both the specific heat and the thermal conductivity are consistent with the concept of guest atoms ''rattling'' in oversized host cages, leading to low thermal conductivities (''phonon glasses''). However, the electron mobilities are quite low, which, if intrinsic, would question the properties of an ''electron crystal'', commonly presumed in ''filled-cage'' materials. The dimensionless thermoelectric figure of merit reaches values of 0.01 at 100 K.

DOI: 10.1103/PhysRevB.64.214404 PACS number(s): 75.50.Cc, 72.20.Pa, 61.48.+c

I. INTRODUCTION

Clathrates are solids made up of large cages of silicon, germanium, or tin (or, in the well-known gas hydrates, of H_2O) that encapsulate guest atoms. All cages are tightly joined, their constituent atoms being tetrahedrally (sp^3-like) bonded. Until recently, clathrates with mostly two different structure types (I and II) have been reported. From these, a large variety of materials can be created by partial substitution of cage atoms and/or by introducing guest atoms into the cages.

The bonding situation of clathrates may, in a first approximation, be understood in terms of the Zintl concept.[1] The more electropositive guest atoms donate electrons to the more electronegative cage (or host) atoms such that the cage atoms complete their valence requirements (octet rule) and build a covalently bonded cage structure. The guest atoms, on the other hand, are ionically bonded to the host framework. Since in this way all valence electrons are used in covalent bonds, one might expect clathrates to be semiconductors. In reality, the situation is more complex and semiconducting clathrates appear to be rather an exception than the rule.

The claim of Slack[2] that clathrates containing guest atoms are promising thermoelectric materials encouraged a number of groups worldwide to work on this topic. He proposed that clathrates behave as ''phonon glasses and electron crystals'': Atoms located in oversized atomic cages are believed to undergo large local anharmonic vibrations, somewhat independent of the other atoms in the crystal. This ''rattling'' may resonantly scatter acoustic-mode, heat-carrying phonons and thus lead to very low and ''glasslike'' thermal conductivities κ (''phonon glasses''). Supposing that κ is phonon dominated, this will increase the thermoelectric figure of merit, $Z=S^2\sigma/\kappa$, only if the charge carriers (and therefore also the electrical conductivity σ) are much less affected by the rattling than the heat-carrying phonons and thus behave as electrons in a crystalline lattice (''electron crystals'').

Our hope is that by introducing suitable rare-earth elements with an unstable $4f$ shell as guest atoms into an adequate semiconducting host framework, a narrow-gap semiconductor (''Kondo insulator''[3]) may be obtained. This would not only be exciting in view of the expected good thermoelectric properties (in addition to the above-discussed low κ values for clathrates, one expects large thermopower S values for Kondo insulators), but also because strongly correlated electron phenomena could be studied in a completely new system, which is quite different from all Kondo insulators known so far.

Up to now we have focused our studies on Ge-containing clathrates. To our knowledge, the only clathrate where a 100% occupation of the guest sites by a rare-earth element is found is $Eu_8Ga_{16}Ge_{30}$. In Refs. 4, 5, and 6, this compound was shown to crystallize in the clathrate-I structure. Our investigations, however, reveal that $Eu_8Ga_{16}Ge_{30}$ exists in *two* modifications, the second one being of the so-called clathrate-VIII structure.[7] Both $Eu_8Ga_{16}Ge_{30}$ modifications, which we shall refer to as the β and α phase, respectively, order ferromagnetically. We are currently trying to modify the Ga-Ge framework in order to suppress the magnetic order and to establish a heavy-fermion semiconducting or Kondo-insulating state.

II. SAMPLE PREPARATION AND STRUCTURAL ANALYSIS

$Eu_8Ga_{16}Ge_{30}$ was prepared from the elements by melting them in a high frequency (HF) furnace under argon atmosphere. The elements were placed, with the atomic ratio Eu:Ga:Ge=8:16:30 (Eu, 99.9 mass%, Lamprecht, further distilled in vacuum; Ga, 99.999 99 mass%, Chempur; Ge, 99.999 mass%, ABCR), into an open glassy-carbon crucible, which was positioned in a quartz tube inside the coil of the HF furnace. The crucible was slowly heated to a maximum temperature of about 950 °C, cooled down to about 750 °C, and then cooled to room temperature. The x-ray diffraction pattern of the as-cast sample showed that the majority phase (about 95%) has a clathrate-I-type structure with a primitive unit cell. In order to get a single-phase sample, annealing for 4 days at 687 °C was performed. Inspection of the x-ray diffraction pattern of the annealed sample revealed that the

TABLE I. Selected crystallographic data (293 K).

Compound	α-$Eu_8Ga_{16}Ge_{30}$	β-$Eu_8Ga_{16}Ge_{30}$
Structure type	$Ba_8Ga_{16}Sn_{30}$ (clathrate-VIII)	clathrate-I
Crystal	gray metallic fragment, size 0.10×0.09×0.03 mm	gray metallic fragment, size 0.09×0.05×0.03 mm
Molar mass	4508.9 amu	4508.9 amu
Space group; formula units	$I\bar{4}3m$ (No. 217); $Z = 1$	$Pm\bar{3}n$ (No. 223); $Z = 1$
Pearson code	*cI*54	*cP*54
Unit cell dimensions [powder, Huber image plate Guinier camera, internal standard LaB_6, $a = 4.15695(6)$ Å]	$a = 10.6281(2)$ Å, $V = 1200.51(4)$ Å^3; 45 reflections ($20° < 2\theta < 99°$), $\lambda(CuK_{\alpha 1}) = 1.540598$ Å	$a = 10.7056(2)$ Å, $V = 1226.97(4)$ Å^3; 60 reflections ($18° < 2\theta < 98°$), $\lambda(CuK_{\alpha 1}) = 1.540598$ Å
Data collection [single crystal, Stoe IPDS]	220 exposures, $\Delta\phi = 1°$; $4° < 2\theta < 48°$, $\lambda(AgK_\alpha) = 0.56087$ Å	250 exposures, $\Delta\phi = 0.8$; $4° < 2\theta < 48°$, $\lambda(AgK_\alpha) = 0.56087$ Å
Data correction	numerical absorption correction, $\mu = 19.7$ mm^{-1}; min. and max. transmission: 0.206, 0.411	numerical absorption correction, $\mu = 19.3$ mm^{-1}; min. and max. transmission: 0.177, 0.512
Structure refinement	SHELXL-97 (16 variable parameters)	SHELXL-97 (21 variable parameters)
$N(hkl)$ measured / unique	6820, 386	14293, 377
$N'(hkl)$ with $I > 2\cdot\sigma(I)$	304	250
$R_{gt}(F)$, $wR_{gt}(F^2)$	0.038, 0.046 ($I > 2\cdot\sigma(I)$)	0.032, 0.063 ($I > 2\cdot\sigma(I)$)
$R_{all}(F)$, $wR_{all}(F^2)$	0.066, 0.051	0.060, 0.067

sample was indeed single phased, but the unit cell was now body-centered cubic and somewhat smaller. Thus, another structural modification of $Eu_8Ga_{16}Ge_{30}$ [isotypic to $Ba_8Ga_{16}Sn_{30}$ (Ref. 8)] had been discovered, representing a low-temperature or so-called α modification. The differential thermal analysis (DTA) revealed that the phase transformation takes place at about 696 °C and that the high-temperature or β modification exists in a range of only 3 °C, melting congruently at 699 °C. Single-phase samples of this β modification were obtained by annealing for 14 days at 697 °C. Crystallographic data of both modifications are summarized in Table I.

$Eu_8Ga_{16}Ge_{30}$ coexists with, at least, two ternary phases of approximate compositions $EuGa_xGe_{6-x}$ ($x \approx 2$) and $Eu_3Ga_xGe_{10-x}$ ($x \approx 4$). To obtain pure α- and β-phase polycrystalline samples, the $Eu_8Ga_{16}Ge_{30}$ ingots were quenched in water after annealing at adequate temperatures. Both x-ray powder diffractometry and optical metallography showed no traces of foreign phases. The chemical analysis (inductively coupled plasma method) of a single-phase sample of α-$Eu_8Ga_{16}Ge_{30}$ annealed at 687 °C gave the composition $Eu_{7.9(1)}Ga_{16.0(1)}Ge_{30.1(2)}$. Both forms of $Eu_8Ga_{16}Ge_{30}$ are gray with metallic luster and are stable in air. The α form is more brittle than the β form. The measured values of the Vickers microhardness of the α and β forms are 330 H_v and 470 H_v, respectively. The densities, measured on fragments of the samples used for the transport measurements, are 6.3(1) and 6.2(1) g/cm^3 for the α and β modification, respectively. Thus, within the experimental uncertainty, no deviation from the ideal densities of 6.24 and 6.10 g/cm^3 could be found. The grain sizes of the samples used for the transport measurements were determined optically on etched surfaces. Most parts of the α-phase sample have an average grain size of 4(2) μm, but several regions have larger crystallites with diameters of up to 60 μm. The crystallites of the β-phase sample are elongated, with lengths of 400–850 μm and widths of 150–440 μm.

The structures of α- and β-$Eu_8Ga_{16}Ge_{30}$, as determined from single-crystal x-ray intensity data collected on a Stoe IPDS diffractometer at room temperature, are depicted in Fig. 1. The structures were refined using the full-matrix least-squares program[9] SHELXL and the atomic coordinates of $Ba_8Ga_{16}Sn_{30}$ and $Sr_8Ga_{16}Ge_{30}$,[8] respectively, as starting values. Both structures are characterized by covalent E_{46} networks (E=Ga, Ge) of fourfold bonded (4*b*) E atoms with polyhedral cages occupied by Eu atoms. The β phase has two kinds of polyhedral cages: E_{20} pentagonal dodecahedra centered by Eu1 and E_{24} tetrakaidecahedra centered by Eu2. There are two Eu1 (2*a* sites) and six Eu2 (6*d* sites) atoms per $Eu_8Ga_{16}Ge_{30}$ formula unit. The α phase has only one type of cage centered by Eu (8*c* site). This cage can be described as a distorted E_{20+3} polyhedron, derived from a E_{20} pentagonal dodecahedron by breaking three E-E bonds and creating nine new ones by adding three more E atoms. In the α phase, the point configuration of the Eu sites ($I4xxx$) can be derived from that of a primitive cubic P_2 point configuration [P_2 ($\frac{1}{4}$ $\frac{1}{4}$ $\frac{1}{4}$)] by deformation in such a way that around each 2*a* 000 site, instead of a cube, a four-capped tetrahedron (''stella quadrangula'') is formed. The central Eu_4 tetrahedron has 5.590-Å-long edges and the Eu caps lie at a distance of 5.652 Åfrom the vertices of the central Eu_4 tetrahedron. Characteristic for the β phase is the nonintersecting three-fold rod packing formed by the Eu2 sites along

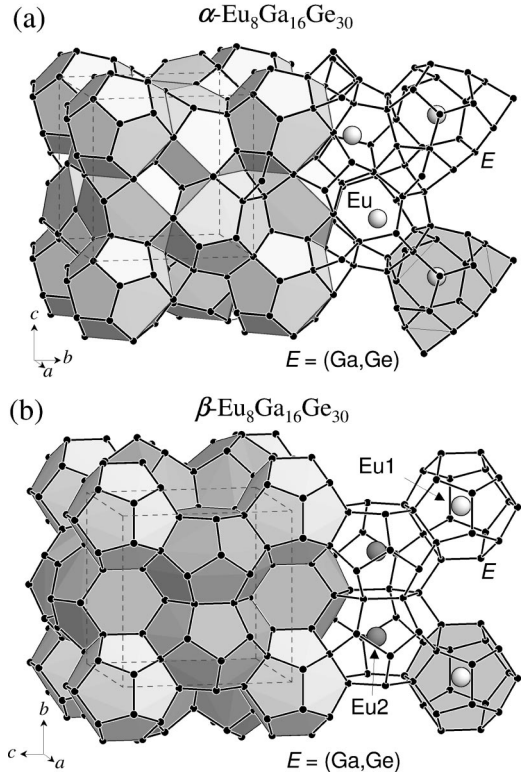

FIG. 1. Crystal structures of α- and β-$Eu_8Ga_{16}Ge_{30}$.

the $\langle 100 \rangle$ directions. The atomic coordinates and the anisotropic atomic-displacement parameters of α- and β-$Eu_8Ga_{16}Ge_{30}$ and of $Ba_8Ga_{16}Ge_{30}$ are given in Table II. The displacement ellipsoid of the Eu2 atoms in the β phase is platelike and a better description can be obtained by replacing each Eu2 ($6d$) site with a Eu2′ ($24k$) site with a quarter occupation. Unlike in Ref. 8, we used this split-site model also for the structure refinement of $Ba_8Ga_{16}Ge_{30}$. In the α phase, however, the displacement ellipsoid of the Eu atoms is much less flattened than that of the Eu2 atoms in the β phase. Therefore, no split sites were introduced.

Since Ga and Ge cannot be distinguished by x rays, we assumed in our structure refinements that the Ga and Ge atoms are randomly distributed among the E sites. However, a short $E2$-$E2$ bond (2.449 Å) in the β phase may indicate a preferential occupation of the $E2$ sites with Ge atoms. All other E-E bond lengths are in the range 2.471–2.503 Å, consistent with a rather random distribution of the Ga and Ge atoms. A comparison of the shortest E-E distances in α- and β-$Eu_8Ga_{16}Ge_{30}$ with the corresponding values determined for $Sr_8Ga_{16}Ge_{30}$ and $Ba_8Ga_{16}Ge_{30}$ is given in Table III. The shortest Eu-Eu distance in α-$Eu_8Ga_{16}Ge_{30}$ is 5.562 Å. In β-$Eu_8Ga_{16}Ge_{30}$ it is, with 5.23 Å, distinctly shorter. The average distance between Eu and the E atoms of the surrounding cage is 3.633 Å for α-$Eu_8Ga_{16}Ge_{30}$. For β-$Eu_8Ga_{16}Ge_{30}$ the average Eu1-E and Eu2-E distances are 3.482 and 3.846 Å, respectively. A compilation of important Eu-Eu and Eu-E distances is given in Table IV.

III. EXPERIMENTAL

We have measured the electrical resistivity ρ, the magnetoresistance, the Hall coefficient R_H, the thermopower S, the thermal conductivity κ, the specific heat C_p, the magnetic susceptibility χ, and the magnetization M in varying temperature (2–400 K) and magnetic-field (0–13 T) ranges for both α- and β-$Eu_8Ga_{16}Ge_{30}$. All electrical transport measurements were done using a standard four-point ac technique. For the thermal transport measurements the usual steady-state method was employed. The specific heat was obtained by using a 2τ-relaxation-type method, and the magnetic measurements were done utilizing a superconducting quantum interference device magnetometer.

IV. RESULTS AND DISCUSSION

Investigation of physical properties reported so far on $Eu_8Ga_{16}Ge_{30}$ was through measurements of the thermal conductivity, thermopower, and electrical resistivity,[5] as well as Raman scattering[10] and neutron diffraction,[6] all on β-phase samples.

In Fig. 2 we show the temperature dependences of the electrical resistivity $\rho(T)$ for both an α- and a β-phase sample of $Eu_8Ga_{16}Ge_{30}$. The room-temperature values of $\rho(T)$ are with 760 and 630 $\mu\Omega$ cm for the α- and β-phase sample, respectively, distinctly smaller than for the (β-phase) sample reported in Ref. 5. The overall temperature dependence of our samples is metallic (positive $d\rho/dT$). However, pronounced anomalies are preceded by a negative $d\rho/dT$, with maximum absolute values at 9.6 and 37 K for the α- and β-phase sample, respectively (cf. inset of Fig. 2). These anomalies are indicative of magnetic phase transitions. The negative $d\rho/dT$ may be due to scattering from critical fluctuations above the phase-transition temperatures. Our observation of these anomalies is in contrast to previous results[5] where the $\rho(T)$ data of a (β-phase) $Eu_8Ga_{16}Ge_{30}$ sample show no sign of a phase transition. Our magnetic and thermal measurements, to be presented below, however, prove that the magnetic phase transitions are intrinsic and ferromagnetic in nature.

The Hall coefficient of both $Eu_8Ga_{16}Ge_{30}$ samples and of $Ba_8Ga_{16}Ge_{30}$ was measured between 2 and 300 K in magnetic fields up to 13 T. The temperature dependences of the Hall coefficient $R_H(T)$, of α- and β-$Eu_8Ga_{16}Ge_{30}$ at 13 T are shown in Fig. 3. For the α-phase sample, $R_H(T)$ changes slightly from -16×10^{-9} m^3/C at 2 K to -15.1×10^{-9} m^3/C at room temperature corresponding, in a one-band model, to 0.47 and 0.49 electrons per $Eu_8Ga_{16}Ge_{30}$ formula unit (3.9 and 4.1×10^{20} cm^{-3}), respectively. For the β-phase sample, $R_H(T)$ varies nonmonotonically with temperature and is -3.2×10^{-9} m^3/C at 2 K and -3.8×10^{-9} m^3/C at 300 K corresponding, in a one-band model, to 2.4 and 2.0 electrons per $Eu_8Ga_{16}Ge_{30}$ formula unit (2.0 and 1.7×10^{21} cm^{-3}), respectively. For $Ba_8Ga_{16}Ge_{30}$, $R_H(T)$ varies smoothly between -12.1×10^{-9} m^3/C at 2 K and -11.4×10^{-9} m^3/C at 300 K corresponding, within the one-band model, to concentrations of 0.64 and 0.68 electrons

TABLE II. Atomic coordinates (Å) and anisotropic-displacement parameters (Å^2) at $T=293$ K (standard deviations in parentheses) for α-$Eu_8Ga_{16}Ge_{30}$ in (a), β-$Eu_8Ga_{16}Ge_{30}$ in (b), and $Ba_8Ga_{16}Ge_{30}$ [space group $Pm\bar{3}n$ (No. 223), $a=10.7840(2)$ Å, $Z=1$, $R_{gt}(F)=0.017$ for 351 reflections with $I>2\sigma(I)$; $wR_{all}(F^2)=0.029$ for 378 unique reflections] in (c). $E=0.348$Ga$+0.652$Ge for all E sites.

(a)

Atom	Pos	x	y	z	U_{11}	U_{22}	U_{33}	U_{12}	U_{13}	U_{23}	U_{eq}
Eu	8*c*	0.1860(1)	x	x	0.0459(5)	U_{11}	U_{11}	–0.0141(4)	U_{12}	U_{12}	0.0459(5)
*E*1	12*d*	1/4	1/2	0	0.0122(9)	0.0166(6)	U_{22}	0	0	0	0.0152(4)
*E*2	2*a*	0	0	0	0.013(1)	U_{11}	U_{11}	0	0	0	0.013(1)
*E*3	24*g*	0.41596(9)	x	0.1441(1)	0.0134(4)	U_{11}	0.0119(6)	–0.0010(6)	0.0008(4)	U_{13}	0.0129(3)
*E*4	8*c*	0.3652(1)	x	x	0.0115(4)	U_{11}	U_{11}	–0.0011(6)	U_{12}	U_{12}	0.0115(4)

(b)

Atom	Pos	x	y	z	U_{11}	U_{22}	U_{33}	U_{12}	U_{13}	U_{23}	U_{eq}
Eu1	2*a*	0	0	0	0.0166(4)	U_{11}	U_{11}	0	0	0	0.0166(4)
Eu2' [a]	24*k*	0.2441(9)	1/2	–0.0413(4)	0.021(2)	0.069(3)	0.046(2)	0	–0.005(3)	0	0.045(1)
*E*1	6*c*	1/4	0	1/2	0.011(1)	0.0108(6)	U_{22}	0	0	0	0.0110(5)
*E*2	16*i*	0.18396(6)	x	x	0.0097(3)	U_{11}	U_{11}	–0.0009(3)	U_{12}	U_{12}	0.0097(3)
*E*3	24*k*	0	0.3092(1)	0.1169(1)	0.0115(5)	0.0096(5)	0.0099(5)	0	0	–0.0012(4)	0.0103(2)
Eu2	6*d*	1/4	1/2	0	0.021(2)	0.195(4)	U_{22}	0	0	0	0.137(3)

(c)

Atom	Pos	x	y	z	U_{11}	U_{22}	U_{33}	U_{12}	U_{13}	U_{23}	U_{eq}
Ba1	2*a*	0	0	0	0.0076(2)	U_{11}	U_{11}	0	0	0	0.0076(2)
Ba2' [a]	24*k*	0.2441(9)	1/2	–0.0413(4)	0.014(1)	0.028(2)	0.022(2)	0	–0.000(7)	0	0.021(1)
*E*1	6*c*	1/4	0	1/2	0.0082(3)	0.0062(2)	U_{22}	0	0	0	0.0069(2)
*E*2	16*i*	0.18452(2)	x	x	0.0059(1)	U_{11}	U_{11}	–0.0008(1)	U_{12}	U_{12}	0.0059(1)
*E*3	24*k*	0	0.30843(3)	0.11813(3)	0.0072(2)	0.0059(2)	0.0064(2)	0	0	–0.0007(1)	0.0065(1)
Ba2	6*d*	1/4	1/2	0	0.0139(2)	0.0482(3)	U_{22}	0	0	0	0.0368(2)

[a] Eu2' (Ba2') is the split position of Eu2 (Ba2); occupancy = 0.25.

TABLE III. Shortest interatomic *E*-*E* distances (Å) for α-$Eu_8Ga_{16}Ge_{30}$, β-$Eu_8Ga_{16}Ge_{30}$, $Sr_8Ga_{16}Ge_{30}$ (Ref. 24), and $Ba_8Ga_{16}Ge_{30}$.

α-$Eu_8Ga_{16}Ge_{30}$			β-$Eu_8Ga_{16}Ge_{30}$			$Sr_8Ga_{16}Ge_{30}$			$Ba_8Ga_{16}Ge_{30}$		
		d_{ave}			d_{ave}			d_{ave}			d_{ave}
E(1) – 4*E*(3)	2.501(1)	2.501	*E*(1) – 4*E*(3)	2.490(1)	2.490	*E*(1) – 4*E*(3)	2.497(0)	2.497	*E*(1) – 4*E*(3)	2.508(0)	2.508
E(2) – 4*E*(4)	2.481(1)	2.481	*E*(2) – *E*(2)	2.449(2)	2.478	*E*(2) – *E*(2)	2.448(1)	2.482	*E*(2) – *E*(2)	2.446(1)	2.488
			3*E*(3)	2.488(1)		3*E*(3)	2.493(0)		3E(3)	2.502(0)	
E(3) – *E*(4)	2.471(2)	2.500									
2*E*(1)	2.501(1)		*E*(3) – 2*E*(2)	2.488(1)	2.492	*E*(3) – 2*E*(2)	2.493(0)	2.499	*E*(3) – 2*E*(2)	2.502(0)	2.515
E(3)	2.526(1)		*E*(1)	2.490(1)		*E*(1)	2.497(1)		*E*(1)	2.508(0)	
			E(3)	2.503(2)		*E*(3)	2.513(0)		*E*(3)	2.548(1)	
E(4) – 3*E*(3)	2.471(1)	2.474									
E(2)	2.481(2)										

TABLE IV. Shortest interatomic *E*-Eu and Eu-Eu distances (Å).

α-$Eu_8Ga_{16}Ge_{30}$			β-$Eu_8Ga_{16}Ge_{30}$				
Eu –	6*E*(1)	3.938(1)	Eu(1) –	8*E*(2)	3.411(1)		5.624(3)
	E(2)	3.423(1)		12*E*(3)	3.539(1)	Eu(1) –12Eu(2) 5.945(0)	5.973(4)
	3*E*(3)	3.486(2)					6.410(4)
	6*E*(3)	3.560(2)	Eu(2) –	4*E*(1)	3.785(0)		
	E(4)	3.300(2)		8*E*(2)	3.978(1)		5.624(3)
	3*E*(4)	3.495(2)		8*E*(3)	3.592(1)	Eu(2)– 4Eu(1) 5.985(0)	5.973(4)
	3*E*(3)	5.104(2)		4*E*(3)	4.150(1)		6.410(4)
Eu –	3Eu	5.562(2)	Eu(2')–	*E*(1)	3.438(8)		5.23(1)
	3Eu	5.590(2)		2*E*(1)	3.856(7)	2Eu(2) 5.353(0)	5.30(1)
	3Eu	5.652(2)		*E*(1)	4.068(7)		5.39(1)
	6Eu	7.758(2)		2*E*(2)	3.623(4)		
				2*E*(2)	3.768(2)		5.799(7)
				2*E*(2)	4.204(3)		6.028(6)
				2*E*(2)	4.371(3)		6.262(6)
				2*E*(3)	3.411(8)		6.400(6)
				2*E*(3)	3.414(7)	8Eu(2) 6.556(0)	6.504(7)
				E(3)	3.704(4)		6.638(5)
				2*E*(3)	3.724(7)		6.767(6)
				2*E*(3)	4.183(2)		6.993(7)
				E(3)	4.579(4)		7.100(6)
							7.249(7)

per $Ba_8Ga_{16}Ge_{30}$ formula unit (5.2 and 5.5×10^{20} cm^{-3}), respectively. While for $Ba_8Ga_{16}Ge_{30}$ the Hall resistivity ρ_H is a linear function of the magnetic field, for both α- and β-$Eu_8Ga_{16}Ge_{30}$ the ρ_H vs H curves are nonlinear at temperatures below T_C. In the following, we analyze these nonlinear $\rho_H(H)$ curves in terms of the anomalous Hall effect.

The anomalous Hall effect arises from the spin-orbit coupling between localized moments and itinerant electrons, which produces an extra electric field with the same orientation as that induced by the Lorentz force in the normal Hall effect. The Hall resistivity of such a material can be written as[11,12] $\rho_H(B)=R_0B+R_s\mu_0M(B)$, where R_0 and R_s are the normal and the spontaneous Hall coefficients, respectively, μ_0 is the vacuum permeability, and M the sample's volume magnetization. Thus $R_H(B)=\rho_H(B)/B$ should be a linear function of $M(B)/B$. That this relation holds for both α- and β-$Eu_8Ga_{16}Ge_{30}$ is shown in Fig. 4. The values of the normal Hall coefficient R_0, which correspond to the intercept of these linear fits, are displayed in Fig. 3 by the full symbols. For the α-phase sample the correction is quite small (below 5%), but for the β-phase sample it is rather important (up to 70%). The value of R_0 at 2 K corresponds to an electron concentration of 3.8×10^{20} cm^{-3} (12.5×10^{20} cm^{-3}) or to 0.46 (1.5) electrons per $Eu_8Ga_{16}Ge_{30}$ formula unit for the

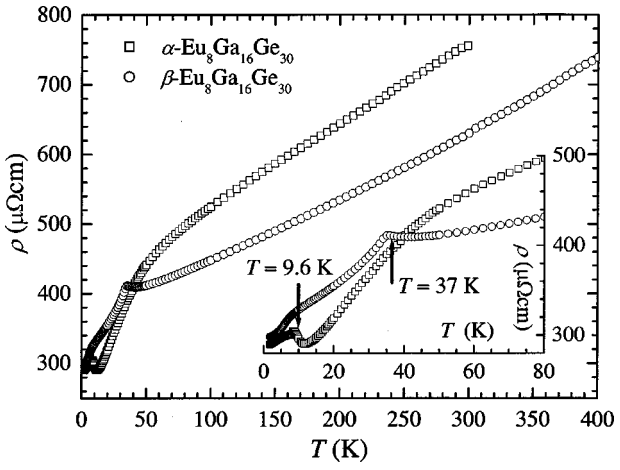

FIG. 2. Temperature dependences of the electrical resistivity $\rho(T)$ of α- and β-$Eu_8Ga_{16}Ge_{30}$. The inset shows a closeup of the low-temperature data.

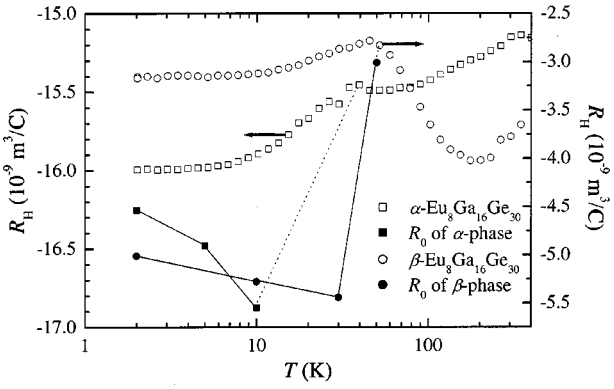

FIG. 3. Temperature dependences of the Hall coefficient R_H at 13 T of α- and β-$Eu_8Ga_{16}Ge_{30}$. The values of the normal Hall coefficient R_0 (R_H corrected for the anomalous Hall effect) are plotted as full symbols. Lines are to guide the eyes.

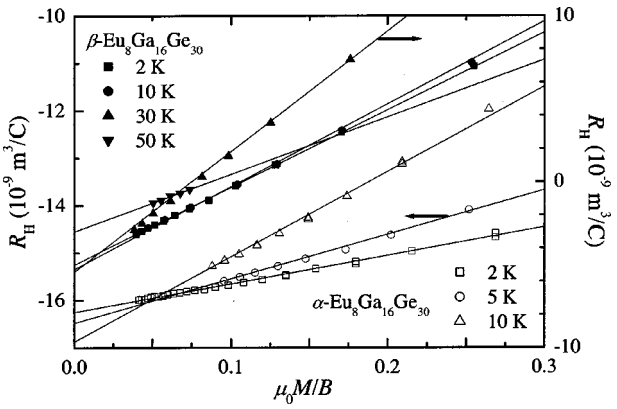

FIG. 4. $R_H(B)=\rho_H(B)/B$ plotted vs $\mu_0 M(B)/B$ for both α- and β-$Eu_8Ga_{16}Ge_{30}$. Linear behavior with the intercept corresponding to R_0 and the slope corresponding to R_s is expected in the presence of an anomalous Hall effect (cf. text).

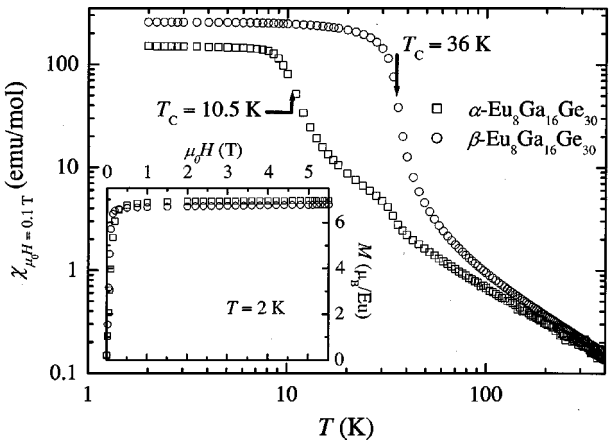

FIG. 5. Magnetic susceptibilities χ of α- and β-$Eu_8Ga_{16}Ge_{30}$, measured in a magnetic field of 0.1 T as a function of temperature T. The inset shows magnetization vs field, $M(H)$, curves at 2 K.

α-phase sample (β-phase sample). The ratio R_s/R_0 is smaller than 1 for the α-phase sample, a value typical for ferromagnetic semiconductors. For the β-phase sample, R_s/R_0 is of the order of 10, a value between those typical for ferromagnetic semiconductors and ferromagnetic metals.[13] The charge-carrier concentrations of both the α- and the β-phase sample are low when compared to simple metals. Even so, they correspond to a substantial deviation from zero as postulated by the Zintl rule.[1] It remains to be clarified whether the charge carriers are intrinsic to $Eu_8Ga_{16}Ge_{30}$ or result from a slight off-stoichiometry of the samples investigated here. A composition $Eu_8Ga_{15.54}Ge_{30.46}$ would, for example, result in the 0.46 electrons per formula unit found for the α-phase sample at 2 K. The Hall mobilities estimated from the R_H data, corrected for the anomalous Hall effect, and from the electrical-resistivity data of Fig. 2 are relatively low, with 58 and 17 $cm^2/V\,s$ at 2 K, and 20 and 7 $cm^2/[V\,s$ at 300 K for the α- and β-phase sample, respectively. This means that the charge carriers are either strongly scattered (large scattering rates) or that they have enhanced effective masses, m^*. Large scattering rates can have various origins. In heavily doped semiconductors, e.g., scattering from the impurities, results in mobilities comparable to those found for $Eu_8Ga_{16}Ge_{30}$. This raises the question whether samples with improved quality have lower carrier concentrations and higher mobilities. An intrinsic source of large scattering rates in $Eu_8Ga_{16}Ge_{30}$ could be the disorder introduced by Ga on the Ge framework.[6] To check for the possibility of enhanced effective masses, calorimetric measurements should be extended to lower temperatures to obtain a better estimate of the electronic specific heat. For $Ba_8Ga_{16}Ge_{30}$, where no magnetic contribution covers the low-temperature behavior, the effective mass is of the order 1. However, a non-negligible interaction between the charge carriers and the anharmonic vibrations of the guest atoms, leading to an enhanced m^*, may not be excluded in $Eu_8Ga_{16}Ge_{30}$. In Ba_6Ge_{25}, this interaction was shown to be strong, leading to very small Hall mobilities (0.6 $cm^2/V\,s$ at 2 K).[14,15]

Figure 5 shows the temperature dependences of the magnetic susceptibility $\chi(T)$ of α- and β-$Eu_8Ga_{16}Ge_{30}$, measured in magnetic fields of 0.1 T. At the lowest temperatures, $\chi(T)$ is almost constant but starts to decrease strongly above approximately 8 and 20 K for the α- and β-phase sample, respectively. Upon cooling the samples in zero magnetic field (data not shown), a spontaneous magnetization M builds up at 10.5 and 36 K for the α- and β-phase sample, respectively. This behavior is typical for ferromagnetic phase transitions with Curie temperatures T_C of 10.5 and 36 K. An analysis of the critical behavior of the zero-field magnetization M just above T_C, $M^{-1}\propto(T-T_C)^{\gamma}$, yields the same values for T_C with $\gamma=0.95$ and 0.8 for the α- and β-phase sample, respectively. Well above the phase transitions, $\chi(T)$ has Curie-Weiss-type temperature dependences with effective magnetic moments of $7.8\mu_B$ and $7.9\mu_B$ per Eu ion and with Weiss temperatures of 11 and 34 K for the α- and β-phase sample, respectively. The moments are in good agreement with the moment of $7.9\mu_B$ expected for a free Eu^{2+} ion and the Weiss temperatures are close to the Curie temperatures. The magnetization vs field curves at 2 K (inset of Fig. 5) are typical for soft ferromagnets: $M(B)$ first increases steeply with the field and then saturates to a constant value, the saturation magnetization. Within our experimental resolution ($\approx$10 Oe), no hysteresis was observed. The saturation magnetization of $7\mu_B$ expected for a free Eu^{2+} ion is almost reached for both samples at 2 K and 5.5 T. Thus, both α- and β-$Eu_8Ga_{16}Ge_{30}$ may be classified as local-moment ferromagnets, with Eu being in its Eu^{2+} state in the entire temperature range.

An interesting question is which mechanism may be responsible for the ferromagnetic ordering of $Eu_8Ga_{16}Ge_{30}$. All Eu-Eu distances being larger than 5.23 Å (Table IV) excludes the direct exchange interaction between the localized $4f$ moments. The indirect exchange interaction between $4f$ moments via the charge carriers is much more long ranged and must be responsible for the ferromagnetism. In this Ruderman-Kittel-Kasuya-Yoshida (RKKY) formalism, the conduction-electron spin polarization around a localized moment has an oscillatory component, the period of which depends on the charge-carrier concentration. The fact that the interaction is ferromagnetic strongly suggests that the second

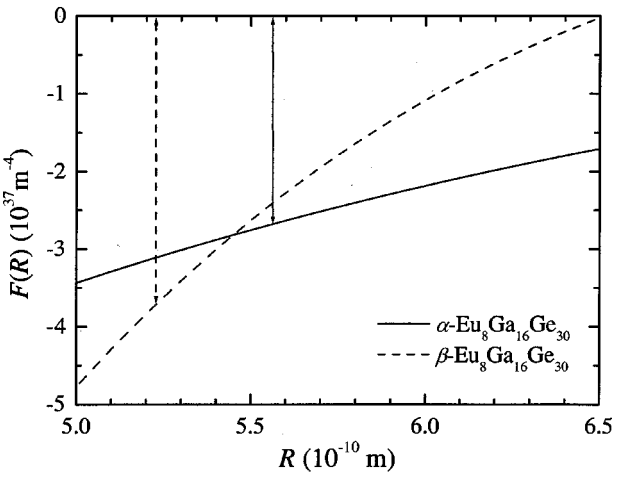

FIG. 6. $F(R)=[2k_FR\cos(2k_FR)-\sin(2k_FR)]/R^4$ of α- and β-$Eu_8Ga_{16}Ge_{30}$ at the respective Curie temperatures. The vertical lines are placed at the shortest Eu-Eu distances.

magnetic moment lies within the first oscillation of the RKKY function around a given moment. A long period of this function is, of course, in agreement with a small charge-carrier concentration. Using the standard formulation for the exchange Hamiltonian,[16] we write $H_{ex}=C\Sigma_{i,j}F(R_{i,j})S_iS_j$ with $F(R)=[2k_FR\cos(2k_FR)-\sin(2k_FR)]/R^4$, and estimate, using the charge-carrier concentrations at T_C determined from the Hall constants, that the interaction between two $4f$ moments is ferromagnetic at distances smaller than 10 Å for α-$Eu_8Ga_{16}Ge_{30}$ and 6.5 Å for β-$Eu_8Ga_{16}Ge_{30}$. The shortest Eu-Eu distances are 5.562 Å for α-$Eu_8Ga_{16}Ge_{30}$ and 5.23 Å for β-$Eu_8Ga_{16}Ge_{30}$ (taking split sites into account). At these distances, F is, in absolute value, larger for the β- than for the α-phase sample. This is illustrated in Fig. 6, where $F(R)$ is plotted as a function of the distance R from a given magnetic moment with spin S_i. The factor C in H_{ex} is the same for both α- and β-$Eu_8Ga_{16}Ge_{30}$. Thus, the higher absolute value of $F(5.23$ Å) for β- than of

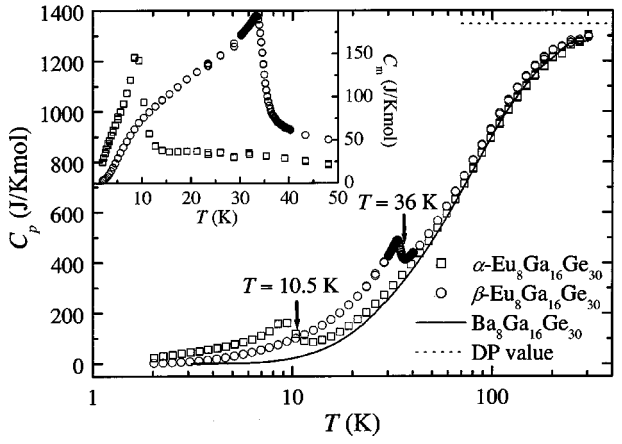

FIG. 7. Temperature dependences of the specific heat $C_p(T)$ of α- and β-$Eu_8Ga_{16}Ge_{30}$. The magnetic contributions $C_m(T)$ of the two modifications, obtained as explained in the text, are shown in the inset.

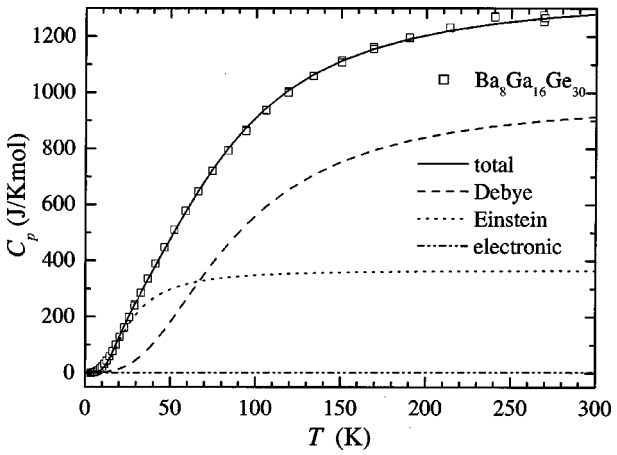

FIG. 8. Temperature dependence of the specific heat $C_p(T)$ of $Ba_8Ga_{16}Ge_{30}$. The total fit and its three contributions (a Debye, an Einstein, and an electronic term), as discussed in the text, are shown.

$F(5.562$ Å) for α-$Eu_8Ga_{16}Ge_{30}$ directly corresponds to a stronger indirect exchange interaction and thus to a higher T_C for the β modification.

The temperature dependences of the specific heat $C_p(T)$ of α- and β-$Eu_8Ga_{16}Ge_{30}$ are shown in Fig. 7. Pronounced λ-type anomalies are observed in the temperature ranges of the ferromagnetic phase transitions discussed above. We have attempted to separate the three contributions to the total specific heat, namely, the lattice contribution $C_L(T)$, the electronic contribution $C_e(T)$, and the magnetic contribution $C_m(T)$. In a first approximation $Ba_8Ga_{16}Ge_{30}$ may be considered as a nonmagnetic reference compound of $Eu_8Ga_{16}Ge_{30}$.

$C_p(T)$ of $Ba_8Ga_{16}Ge_{30}$ is also shown in Fig. 8. A good description of these data is obtained with $C_p(T)=C_L(T)+C_e(T)$. The electronic term is calculated from the Hall coefficient, assuming that the effective mass of the charge carriers is equal to the free-electron mass. This term amounts to 21% of the total specific heat at 3 K and becomes relatively smaller at higher temperatures. The lattice contribution was fitted to the sum of a Debye and an Einstein term. The fit parameters are the Debye temperature Θ_D, the Einstein temperature Θ_E, and the numbers N_D and N_E of Debye and Einstein oscillators per formula unit, taking into account that their sum is 54, the number of atoms per formula unit. We obtain $\Theta_D=355$ K, $\Theta_E=80$ K, $N_D=39$, and $N_E=15$. The total fit and the three contributions, namely, $C_e(T)$ and the Debye and the Einstein contribution to $C_L(T)$, are shown in Fig. 8. Very similar results were obtained for $Sr_8Ga_{16}Ge_{30}$ (data not shown): $\Theta_D=358$ K, $\Theta_E=79$ K, $N_D=38$, and $N_E=16$.

To obtain the magnetic contributions $C_m(T)$ to the total $C_p(T)$ of α- and β-$Eu_8Ga_{16}Ge_{30}$, the lattice contribution of $Ba_8Ga_{16}Ge_{30}$, determined as discussed above, and the electronic contributions of the α- and β-phase sample, respectively, were subtracted from the $C_p(T)$ data. As above, the electronic contributions were estimated from the Hall coefficients, assuming that the effective charge-carrier mass is the free-electron mass. $C_m(T)$ of α- and β-$Eu_8Ga_{16}Ge_{30}$ are

shown in the inset of Fig. 7. The Curie temperatures, determined in a $C_m(T)/T$ plot with an entropy-balancing geometric construction, are in good agreement with those determined from the magnetization measurements. Integrating over $C_m(T)/T$ up to T_C yields magnetic entropies of 15.4 and 24.9 J/K per mole Eu for the α- and β-phase sample, respectively. These values are approximately 90% and 145% of the theoretical value $Rln(2S+1)$ with $S=7/2$, where R is the gas constant. Thus, the magnetic phase transitions observed in both samples are clearly bulk effects and cannot be ascribed to impurities. The relatively poor agreement with the theoretical entropy value is most probably due to $Ba_8Ga_{16}Ge_{30}$ not being a perfect reference system, as will be further outlined below.

In Ref. 17 it was suggested that the rattling of the guest atoms in the cages corresponds to truly localized vibrations. These may be described by a quantized harmonic oscillator (Einstein oscillator). The Einstein frequency of such an oscillator is given by $\omega_E=\sqrt{(K/m)}$, where K is the force constant and m the mass of the rattler. K is larger, the smaller the volume mismatch between the rattler and the cage. The cage atoms, on the other hand, are considered as part of a Debye solid. Considering the structure of $Ba_8Ga_{16}Ge_{30}$, where, per formula unit, two Ba atoms (Ba1 site) are located in E_{20} polyhedra and six Ba atoms (Ba2 site) are located in E_{24} polyhedra, one may expect two different Einstein frequencies, a larger one for the smaller cages and a smaller one for the larger cages. To account for this situation we tried to fit the lattice contribution to the specific heat of $Ba_8Ga_{16}Ge_{30}$ with two sets of Einstein oscillators. However, the number of parameters in the fitting was too large to give meaningful results and the quality of the fit was not improved with respect to the one where just one set of Einstein oscillators was used. Thus, from the specific-heat measurements we have no evidence for the presence of two subsets of Einstein oscillators with distinctly different Einstein frequencies in $Ba_8Ga_{16}Ge_{30}$.

As pointed out in Ref. 18, the atomic-displacement parameters at room temperature may be used to estimate the Einstein temperatures, the Debye temperature, and the room-temperature thermal conductivity of any compound with small static disorder. We have calculated the Debye temperature Θ_D and the Einstein temperatures $\Theta_E=\hbar\omega_E/k_B$ for both Ba sites in $Ba_8Ga_{16}Ge_{30}$, using the isotropic displacement parameters $U_{\rm eq}$ given in Table II. For the Ba2 site, $U_{\rm eq}$ of the split-site Ba2′ was used. We obtain $\Theta_D=300$ K and $\Theta_{E1}=121$ K and $\Theta_{E2}=72$ K for the Ba1 and Ba2 site, respectively. The average Einstein temperature $\Theta_{\rm E,av}=(2\Theta_{E1}+6\Theta_E)/8=84$ K, where 2 and 6 are the multiplicities of the Ba1 and the Ba2 site, is in good agreement with the result of our fit of the lattice specific heat of $Ba_8Ga_{16}Ge_{30}$ discussed above. This indicates that $U_{\rm eq}$ does indeed describe the rattling of the Ba atoms in the cages and that any static-disorder contribution is small. Using the atomic-displacement parameters given in Ref. 8, Θ_E and Θ_D of $Ba_8Ga_{16}Ge_{30}$ were estimated[18] to be 51 and 275 K, respectively. The smaller Θ_E value as compared to our findings may be due to the fact that in Ref. 8, no split positions were introduced for the Ba2 site, i.e., $U_{\rm eq}$(Ba2) contains contributions from both rattling and static disorder.

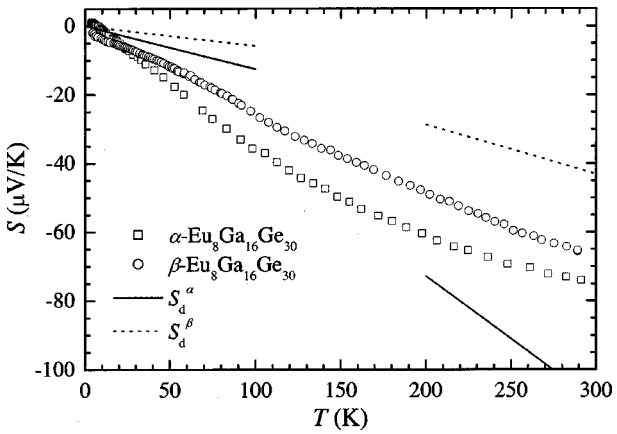

FIG. 9. Temperature dependences of the thermopower $S(T)$ of α- and β-$Eu_8Ga_{16}Ge_{30}$. The low- and higher-temperature limits of the free-electron diffusion thermopower S_d (cf. text) are plotted as straight lines.

For $Eu_8Ga_{16}Ge_{30}$ the Einstein and Debye temperatures estimated from the room-temperature atomic-displacement parameters (Table II) are $\Theta_E=45$ K and $\Theta_D=214$ K for the α-phase sample and $\Theta_{E1}=75$ K, $\Theta_{E2}=45$ K (using the split site Eu2′), and $\Theta_D=245$ K for the β-phase sample. The lattice specific-heat curves, $C_L(T)$, generated from these parameters give only a poor agreement with the measured $C_p(T)$ data. For the β-phase sample we improved the agreement by fitting Θ_D to the data well above the Curie temperature, where $C_e(T)$ and $C_m(T)$ are negligibly small, keeping the Einstein temperatures fixed to the above values. Fitting the Einstein temperatures is not possible due to the large magnetic contribution at temperatures up to approximately 50 K. We obtain $\Theta_D=302$ K. For the α phase sample, on the other hand, we could fit both the Debye and the Einstein temperature using the $C_p(T)$ data above 30 K, where $C_e(T)$ and $C_m(T)$ are negligibly small. Very good agreement with the data is obtained for $\Theta_D=364$ K, $\Theta_E=72$ K, and $N_D=38$ ($N_E=16$). If this fit is taken as a phonon background, the entropy below the $C_m(T)/T$ curve is found to agree well with the theoretical value.

For β-$Eu_8Ga_{16}Ge_{30}$, Raman-scattering experiments have been performed.[10] The vibrational mode that was associated with the guest atoms in the E_{24} polyhedra has a Raman shift of 23 cm^{-1} (33 K), in rough agreement with $\Theta_{E2}=45$ K. The mode associated with guest atoms in the E_{20} polyhedra is not Raman active.

The fact that the fits of the lattice specific heats of $Ba_8Ga_{16}Ge_{30}$ and α-$Eu_8Ga_{16}Ge_{30}$ yield $N_E=15$ and $N_E=16$, respectively, instead of 8 (for the eight guest atoms per formula unit) indicates that making a clear-cut distinction between the guest atoms as Einstein oscillators and the framework atoms as Debye oscillators is oversimplified. This is in agreement with Raman-scattering results[10] that give evidence for a hybridization between some of the rattle modes associated with vibrations of the guest atoms in the E_{24} polyhedra of the clathrate-I structure and low-frequency modes

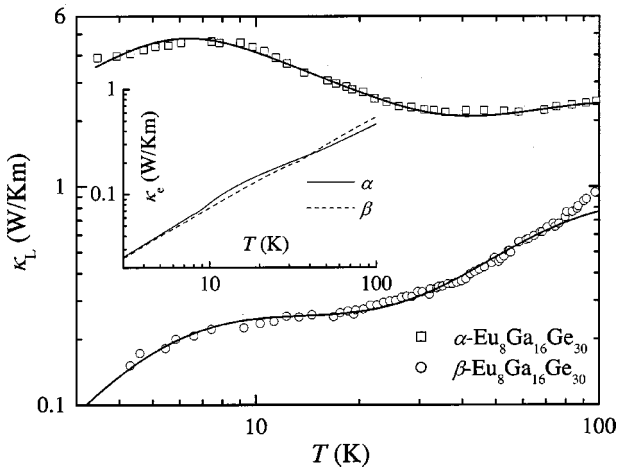

FIG. 10. Temperature dependences of the lattice thermal conductivity $\kappa_L(T)$ of α- and β-$Eu_8Ga_{16}Ge_{30}$ on a double-logarithmic scale. The lines are fits to the data obtained as explained in the text. The inset shows the electronic contributions $\kappa_e(T)$ obtained as explained in the text.

associated with the framework atoms. In addition, optical modes of the clathrate-I framework were calculated[19] to appear with appreciable weight above 90 cm^{-1} (130 K), a frequency that is not too far from the Einstein frequencies of the guest atoms.

The temperature dependence of the thermopower $S(T)$, of both α- and β-$Eu_8Ga_{16}Ge_{30}$ is plotted in Fig. 9. The relatively large negative values of S are in agreement with a relatively small concentration of electronlike charge carriers, as extracted from our Hall-effect measurements. Previously published $S(T)$ data[5] on β-$Eu_8Ga_{16}Ge_{30}$ are qualitatively similar to ours, with an absolute value of S at room temperature twice as large as for our sample, however. The diffusion thermopower is, in the free-electron approximation, given by[20] $S_d=\pi^2k_B^2T/3e\eta$ at very low temperatures and by $S_d=\pi^2k_B^2T/e\eta$ at higher temperatures. η is the Fermi energy, which is related to the charge-carrier concentration. The other symbols have their usual meaning. The straight lines in Fig. 9 are calculated from these relations taking the charge-carrier concentrations at 2 and 300 K. The $S(T)$ data are of the same order as these rough estimates of $S_d(T)$, indicating that the diffusion thermopower is an important contribution to the total thermopower. Undoubtly, there will also be a phonon-drag contribution, $S_g(T)$, but the simple relation[20] $S_g \propto T^3$ does not give a satisfying description of the low-temperature data. We further notice that no significant anomalies are observed at the respective Curie temperatures of both samples. This indicates that both the magnon drag thermopower and the anomalous magnetic thermopower[16] are, most probably, unimportant in $Eu_8Ga_{16}Ge_{30}$.

Figure 10 displays the temperature dependences of the lattice thermal conductivity $\kappa_L(T)$ of both α- and β-$Eu_8Ga_{16}Ge_{30}$ in a semilogarithmic plot. The electronic contribution $\kappa_e(T)$ shown in the inset of Fig. 10, was estimated from the electrical resistivity using the Wiedemann-Franz law, $\kappa_e(T)=\pi^2k_B^2/(3e^2)T/\rho(T)$, and was subtracted from the total measured thermal conductivity. $\kappa_e(T)/\kappa_L(T)$ reaches a maximum of 20% at 100 K for α-$Eu_8Ga_{16}Ge_{30}$, and of 60% at 50 K for β-$Eu_8Ga_{16}Ge_{30}$. In spite of the same composition, both the absolute values and the temperature dependences of $\kappa_L(T)$ are quite different for the two modifications. For β-$Eu_8Ga_{16}Ge_{30}$, $\kappa(T)$ was measured previously.[5] κ_L of our sample is 1.5 times greater at 100 K and decreases more strongly with decreasing temperature than κ_L of the sample of Ref. 5. The overall behavior, however, is similar for both β-phase samples being typical of highly disordered, even amorphous, solids. The origin of this amorphouslike thermal conductivity was discussed in a number of publications.[21] The essence is that the heat-carrying acoustic phonons, which are framework derived, are assumed to be strongly scattered from the anharmonic vibrations of the cage atoms, leading to a dip in the thermal conductivity in the temperature range 4–35 K. While for the sample of Ref. 5 a pronounced dip is observed at approximately 20 K, this feature is much less pronounced for the sample investigated here. In fact, $\kappa_L(T)$ of our β-$Eu_8Ga_{16}Ge_{30}$ sample closely resembles $\kappa(T)$ of amorphous SiO_2.[21] The $\kappa_L(T)$ data of the β-$Eu_8Ga_{16}Ge_{30}$ sample of Ref. 5 were fitted in Ref. 22 to a phenomenological model put forward by Cohn *et al.*[4] In this model, $\kappa_L(T)$ is calculated from the kinetic gas-theory expression $\kappa_L=(v/3)\int_0^{\omega_D}C(\omega)l(\omega)d\omega$ with a Debye specific heat C and, assuming the validity of Matthiessen's rule, a phonon mean free path l that is the sum of terms representing tunneling states (TS), resonant scattering (res), and Rayleigh (R) scattering: $l=(l_{\rm TS}^{-1}+l_{\rm res}^{-1}+l_R^{-1})^{-1}+l_{\rm min}$, with $l_{\rm TS}^{-1}=A(\hbar\omega/k_B)\tanh(\hbar\omega/2k_BT)+(A/2)(k_B/\hbar\omega+B^{-1}T^{-3})^{-1}$, $l_{\rm res}^{-1}=\Sigma_{i=1}^{2}C_i\omega^2T^2/[(\omega_i^2-\omega^2)^2+\gamma_i\omega_i^2\omega^2]$, and $l_R^{-1}=D(\hbar\omega/k_B)^4$. The lower limit on l was assumed to be a constant, $l_{\rm min}$. In Ref. 22 the Debye temperature was fixed to $\Theta_D=270$ K, the average sound velocity to $v=2600$ m/s, and the Einstein temperatures corresponding to the resonant frequencies to $\Theta_{E1}=\hbar\omega_1/k_B=53$ K and $\Theta_{E2}=82$ K. The other parameters, i.e., $l_{\rm min}$, A, B, C_1, C_2, γ_1, γ_2, and D were determined by fitting. We used a slightly different approach. We fixed the Debye temperature to $\Theta_D=302$ K, as determined from the fit of the $C_p(T)$ data of β-$Eu_8Ga_{16}Ge_{30}$ with fixed Einstein temperatures as discussed above. Correspondingly, the sound velocity was fixed to $v=(\Theta_Dk_B/\hbar)/(6\pi^2n)^{1/3}=2873$ m/s, where n is the number of atoms per unit volume. We further fixed the Einstein temperature of the Eu1 site to $\Theta_{E1}=75$ K and of the Eu2 site to $\Theta_{E2}=45$ K, as obtained from the atomic-displacement parameters, and we set $C_2/C_1=3$, corresponding to the ratio of the multiplicities of the Eu2 and Eu1 sites. We further fixed $\gamma_1=\gamma_2=1.5$, which is the value obtained from the fit of the α-$Eu_8Ga_{16}Ge_{30}$ data to be presented below. Fitting the other parameters to the data (cf. solid line in Fig. 10) yields $l_{\rm min}=4.3\times10^{-10}$ m, $A=1.4\times10^5$ m^{-1} K^{-1}, $B=3.9\times10^{-2}$ K^{-2}, $C_1=3.1\times10^{30}$ m^{-1} s^{-2} K^{-2}, and $D=3.3$ m^{-1} K^{-4}. All parameters are in overall agreement with those obtained in Ref. 22 (if the sign error of the exponent of C_1 and C_2 in Ref. 22 is corrected for). For the α-phase sample we set $\Theta_D=364$ K, $v=3396$ m/s, and $\Theta_E=72$ K, as determined from the fit of the $C_p(T)$ data of α-$Eu_8Ga_{16}Ge_{30}$ discussed

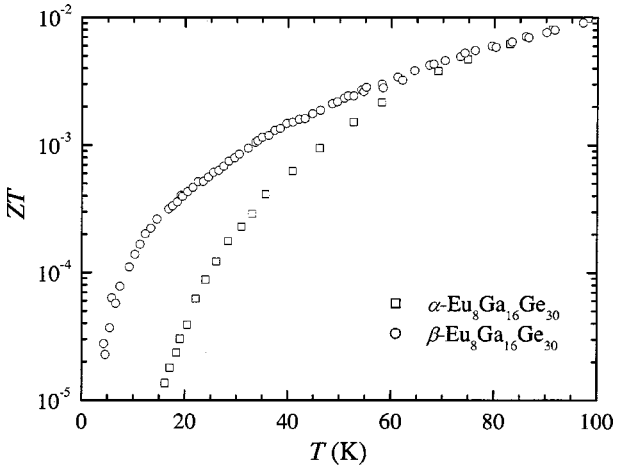

FIG. 11. Temperature dependences of the dimensionless thermoelectric figure of merit, $ZT(T)$, of α- and β-$Eu_8Ga_{16}Ge_{30}$.

above. The best fit to the data (cf. solid line in Fig. 10) is obtained for $l_{min}=3.7\times10^{-10}$ m, $A=2.2\times10^{3}$ m^{-1} K^{-1}, $B=6.0\times10^{-2}$ K^{-2}, $C=3.2\times10^{30}$ $m^{-1}s^{-2}K^{-2}$, $\gamma=1.5$, and $D=0.24$ $m^{-1}K^{-4}$, again a reasonable set of parameters. The ratio A/B, a measure of the density of strongly coupled tunneling states,[22] is much larger for the β- than for the α-phase sample. This is plausible if one assumes that the tunneling states correspond to the static positional disorder induced by the split site Eu2′, which is only present in the β phase. The larger value of D for the β- than for the α-phase sample indicates greater mass-density variations in the former compound. In all, the lattice contributions of the thermal conductivity of both α- and β-$Eu_8Ga_{16}Ge_{30}$ may be well described by a model in which, in addition to mass-density scattering, two scattering mechanisms related to the filled-cage structure are taken into account: The resonant scattering is directly related to the rattling of the guest atoms in the oversized cages and the scattering from tunneling states may be associated with cage atoms tunneling between different split sites.

Finally, we present the dimensionless thermoelectric figure of merit, ZT, as a function of temperature in Fig. 11. ZT increases monotonically with temperature for both samples and reaches values of 0.01 at 100 K.

During the review process of the present paper, a report on various physical properties of $Eu_8Ga_{16}Ge_{30}$ single crystals appeared.[23] In a brief statement, the existence of a second modification (called α phase in the present paper) is announced, in agreement with our findings.

V. PERSPECTIVE

In summary, we have synthesized and investigated the clathrate $Eu_8Ga_{16}Ge_{30}$ in its two modifications, the well-known β phase with the clathrate-I structure and the new α phase with the clathrate-VIII structure. Polycrystalline samples of both phases are local-moment ferromagnets, yet with relatively low Curie temperatures. The temperature dependences of the electrical resistivities are metallic in nature, but the charge-carrier concentrations are quite small, as expected from the charge-balanced Zintl count. The small Hall mobilities might, if intrinsic to $Eu_8Ga_{16}Ge_{30}$, be related to structural disorder on the Ga-Ge framework and/or to a non-negligible interaction between the charge carriers and the rattle modes of the guest atoms. The latter possibility would question the validity of the concept of an electron crystal[2] for $Eu_8Ga_{16}Ge_{30}$. However, measurements on high-quality single crystals are needed to test whether the mobilities in $Eu_8Ga_{16}Ge_{30}$ are indeed intrinsically low. The specific-heat and the thermal-conductivity data provide evidence for the existence of rattling guest atoms and for the strong scattering of heat-carrying acoustic phonons from them, in line with the concept of a phonon glass.[2] The thermopower is negative and appears to be dominated by the diffusion term. The dimensionless figure of merit reaches values of 0.01 at 100 K. In order to improve it, the carrier concentration should be decreased (which should lead to a higher absolute value of the thermopower) and/or the charge-carrier mobilities increased. Currently, we are trying to slightly modify $Eu_8Ga_{16}Ge_{30}$ by both chemical substitutions and application of hydrostatic pressure in order to suppress the ferromagnetism and to promote a strongly correlated semiconducting (Kondo-insulating) state.

ACKNOWLEDGMENTS

We thank H. Borrmann and R. Cardoso Gil for the single-crystal x-ray diffraction and R. Niewa for the DTA measurements. Useful discussions with P. Thalmeier are also acknowledged.

*On leave from W. Trzebiatowski Institute for Low Temperature and Structure Research, Polish Academy of Sciences, 50-950 Wroclaw, Poland.

[1] H. Schäfer, Annu. Rev. Mater. Sci. **15**, 1 (1985).

[2] G. A. Slack, in *CRC Handbook of Thermoelectrics*, edited by D. M. Rowe (Chemical Rubber, Boca Raton, FL, 1995), Chap. 34.

[3] G. Aeppli and Z. Fisk, Comments Condens. Matter Phys. **16**, 155 (1992).

[4] J. L. Cohn, G. S. Nolas, V. Fessatidis, T. H. Metcalf, and G. A. Slack, Phys. Rev. Lett. **82**, 779 (1999).

[5] G. S. Nolas, in *Thermoelectric Materials 1998–The Next Generation Materials for Small-Scale Refrigeration and Power Generation Applications*, edited by T. M. Tritt, H. B. Lyon, Jr., G. Mahan, and M. G. Kanatzidis, Mater. Res. Soc. Symp. Proc. No. 545 (Materials Research Society, Pittsburgh, 1999), p. 435.

[6] B. C. Chakoumakos, B. C. Sales, and D. G. Mandrus, J. Alloys Compd. **322**, 127 (2001).

[7] S. Bobev and S. C. Sevov, J. Am. Chem. Soc. **123**, 3389 (2001).

[8] B. Eisenmann, H. Schäfer, and R. Zahler, J. Less-Common Met. **118**, 43 (1986).

[9] G. M. Sheldrick, SHELXL-97, Program for Crystal Structure Refinement, University of Göttingen, Germany, 1997.

[10] G. S. Nolas and C. A. Kendziora, Phys. Rev. B **62**, 7157 (2000).

[11] E. Arushanov, C. Kloc, H. Hohl, and E. Bucher, J. Appl. Phys. **75**, 5106 (1994).

[12] R. C. O'Handley, in *The Hall Effect and its Applications*, edited

by C. L. Chien and C. R. Westgate (Plenum, New York, 1980).
[13] E. L. Nagaev and E. B. Sokolova, Fiz. Tverd. Tela (Leningrad) **19**, 533 (1977) [Sov. Phys. Solid State **19**, 425 (1977)].
[14] S. Paschen, V. H. Tran, M. Baenitz, W. Carrillo-Cabrera, R. Michalak, Yu. Grin, and F. Steglich, in *Proceedings of the XIX International Conference on Thermoelectrics*, edited by D. M. Rowe (Babrow Press, Wales, United Kingdom, 2000), p. 374.
[15] S. Paschen, V. H. Tran, M. Baenitz, W. Carrillo-Cabrera, Yu. Grin, and F. Steglich (unpublished).
[16] See, e.g., E. Gratz and M. J. Zuckermann, in *Handbook on the Physics and Chemistry of Rare Earths*, edited by K. A. Gschneidner and L. Eyring (North-Holland, Amsterdam, 1982).
[17] V. Keppens, D. Mandrus, B. C. Sales, B. C. Chakoumakos, P. Dai, R. Coldea, M. B. Maple, D. A. Gajewski, E. J. Freeman, and S. Bennington, Nature (London) **395**, 876 (1998).
[18] B. C. Sales, B. C. Chakoumakos, D. Mandrus, and J. W. Sharp, J. Solid State Chem. **146**, 528 (1999).
[19] J. Dong, O. F. Sankey, and C. W. Myles, Phys. Rev. Lett. **86**, 2361 (2001).
[20] F. J. Blatt, P. A. Schroeder, C. L. Foiles, and D. Greig, *Thermoelectric Power of Metals* (Plenum Press, New York, 1976).
[21] For a review see, e.g., G. S. Nolas, G. A. Slack, and S. B. Schujman, Semicond. Semimet. **69**, 255 (2001).
[22] G. S. Nolas, T. J. R. Weakley, J. L. Cohn, and R. Sharma, Phys. Rev. B **61**, 3845 (2000).
[23] B. C. Sales, B. C. Chakoumakos, R. Jin, J. R. Thompson, and D. Mandrus, Phys. Rev. B **63**, 245113 (2001).
[24] W. Carrillo-Cabrera, R. Cardoso Gil, S. Paschen, and Yu. Grin (unpublished).